



FROM RESEARCH TO INDUSTRY

THERMAL SUB-GRID BOUNDARY LAYER MODELLING AROUND BUBBLES AT MODERATE REYNOLDS AND PRANDTL NUMBERS

ICMF (Kobe) – 2023

07/04/2023

M. GROSSO¹ – G. Bois² – A. TOUTANT³

¹ CEA DES/ISAS/DM2S/STMF/LMSF SACLAY (mathis.grosso@cea.fr)

² CEA DES/ISAS/DM2S/STMF/LMSF SACLAY (guillaume.bois@cea.fr)

³ PROMES-CNRS, UNIVERSITÉ DE PERPIGNAN VIA DOMITIA (adrien.toutant@univ-perp.fr)

Introduction

From available methods to a novel approach

LRS methodology

DNS simulations and post-processing tool

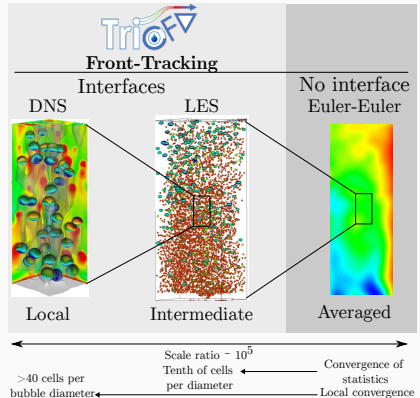
A priori implementation and results

Conclusions and prospects

Upscaling approach for **boiling** investigation

Simulations at three scales:

- **Local** or DNS : Reference data
⇒ **Too costly**
- **Intermediate**: Modelling of strong fluctuations and variations of temperature:
⇒ **Thermal boundary layer modelling**
- **Averaged** (RANS Euler-Euler): Macroscopic closures
⇒ **Interfacial heat transfers for non-resolved interfaces**





Need: A liquid-vapour heat transfer model in bubble swarms

- Heat transfer exchange coefficient (Nusselt number Nu_b) which determines **condensation/evaporation** rate at the interface:

$$Nu_b \propto \int_{\Gamma} \nabla T \cdot \mathbf{n}_{\Gamma}|_{\Gamma} dS$$

$$Nu_b = f \left(Re_b, Pr_l = \frac{\alpha_l}{\nu_l}, \mu_v/\mu_l, \alpha = \frac{\Omega_v}{\Omega_l}, Ja = \frac{\rho_l C_{pl} \Delta T}{\rho_v \mathcal{L}^{vap}} \right) \quad (1)$$

Problem: Capture the strong variations $Nu_b \propto \nabla T \cdot \mathbf{n}_{\Gamma}|_{\Gamma}$ is costly

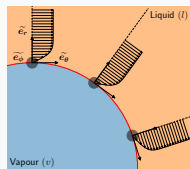
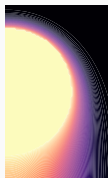
Thermal boundary layer
thickness $\delta \ll D_b$



Separation of scales



Local refinements



Solution: A DNS thermal boundary layer coupling (conceptualisation)

- Keep the **explicit tracking** of the interface (Front-Tracking).
- Enhance the prediction of strong variations on a **finite thickness**.
- Reduce the computational **cost**

Introduction

From available methods to a novel approach

LRS methodology

DNS simulations and post-processing tool

A priori implementation and results

Conclusions and prospects

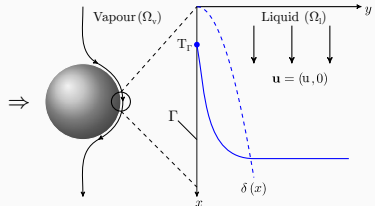
RADIAL/NORMAL TEMPERATURE VARIATIONS ARE EXPECTED TO BE HIGH



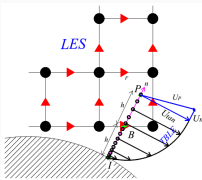
INVESTIGATE A UNI-DIRECTIONAL REFINEMENT APPROACH

Uni-directional refinement approaches

- (1) Fit an analytical form of solution
(Quasi-Static Correction, **QSC**).
⇒ Inspired by of Bothe and Fleckenstein 2013; Weiner and Bothe 2017.
(⇒ **Grosso et al., 2023, in writing.**)
- (2) **Laminar Radial Sub-resolution (LRS)**.
⇒ Current presentation !



Inspiration: Thin/turbulent Boundary Layer Equation (TBLE)



It consists in a **LES-RANS** coupling to solve for near wall turbulence and transfers:

- (1) **Turbulence** on flat plates, channels (Benarafa et al. 2006).
- (2) **Heat transfer** on flat plates, channels by Chatelain 2004.
- (3) Turbulence on **complex geometries** (turbines...) coupled to an Immersed Boundary Method of Bizid 2017.

Introduction

From available methods to a novel approach

LRS methodology

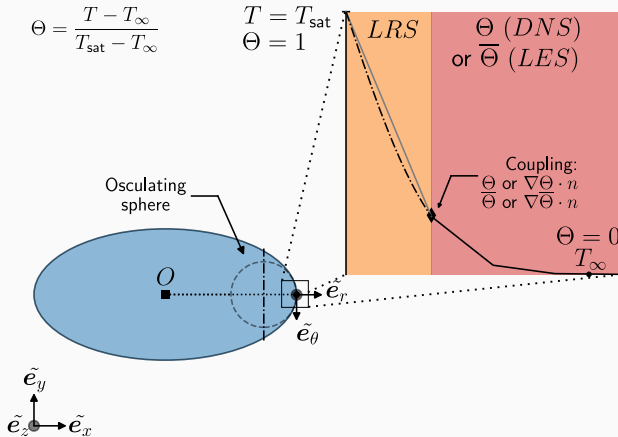
DNS simulations and post-processing tool

A priori implementation and results

Conclusions and prospects

Principles of LRS (Laminar Radial Sub-resolution)

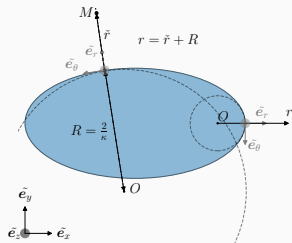
- Solve for each phase temperature **separately**.
- Resolve a **unidirectional** problem in the **osculating spherical basis** for each **interface portion** (Front-Tracking).



Hypotheses

- Interface attached frame of reference $u_r \leftarrow u_r - u_r|_{\Gamma}$.
- Temporal term neglected $\partial_t = 0$ i.e. **quasi-static** approach.
- No azimuthal variations: $\frac{\partial^n \Theta}{\partial \phi^n} = 0, u_\phi = 0$.

Radial advection-diffusion equation in spherical coordinates (2D-axi)



$$\underbrace{\frac{\partial^2 \Theta}{\partial r^2}}_{D^r} + \frac{2}{r} \frac{\partial \Theta}{\partial r} - \underbrace{\frac{u_r}{\alpha_l} \frac{\partial \Theta}{\partial r}}_{C^r} = \underbrace{\frac{u_\theta}{\alpha_l} \frac{1}{r} \frac{\partial \Theta}{\partial \theta}}_{C^\theta} - \underbrace{\frac{1}{r^2} \frac{\partial^2 \Theta}{\partial \theta^2}}_{D^\theta} \quad (2)$$

Source terms

$$\nabla T \cdot \tilde{e}_r \equiv \nabla T \cdot \mathbf{n}_\Gamma$$

Θ : dimensionless temperature
Interpolated values

Introduction

From available methods to a novel approach

LRS methodology

DNS simulations and post-processing tool

A priori implementation and results

Conclusions and prospects

Dimensionless numbers

$$Ar^* = \left(g D_b \frac{\rho_l - \rho_v}{\rho_l} \right)^{1/2} \frac{D_b}{\nu_l}; Pr_l = \frac{\alpha_l}{\nu_l}; Re_b = \frac{U_{term} D_b}{\nu_l}; Ja = \frac{\rho_l C_{pl} \Delta T}{\rho_v \mathcal{L}^{vap}}$$

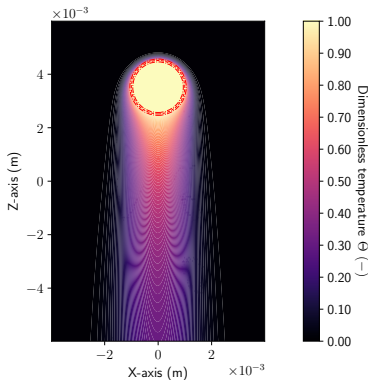
Numerical setup

Hypotheses:

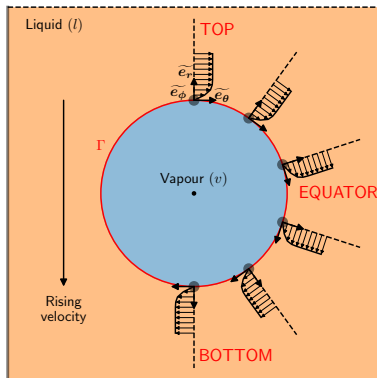
- No phase change $Ja \rightarrow 0$.
- $T_\Gamma = T^{sat}$.
- Outflow boundary conditions $\nabla T \cdot \mathbf{n}_\Omega = 0$.
- Bubble is kept spherical.

Physical parameters range of study:

- $Ar^* \in \{10; 50\}$
- $Pr_l \in \{1; 2.5; 5\}$
- $D_b/\Delta \in [12, 96]$
- Domains sizes:
 $\{[3, 3, 4]; [4, 4, 6]\} \times D_b$



Rising bubble at $Ar^* = 50$,
 $Pr_l = 1$ ($Re_b \approx 62.5$).



Post-process quantities on probes

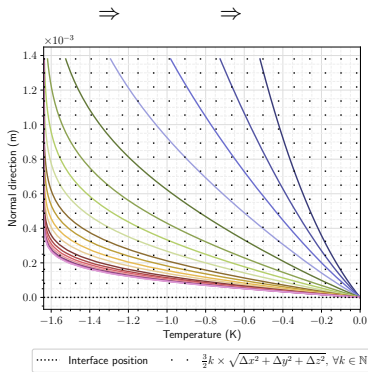
$$\theta_{\text{VISU}} \in [-90, 90]^\circ$$

BOTTOM (1)
 -90°

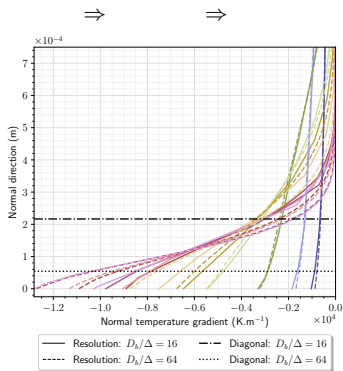
EQUATOR (2)
 0°

TOP (3)
 90°

Local temperature profiles and normal derivative: T and $\nabla T \cdot \tilde{e}_r = \frac{\partial T}{\partial r}$



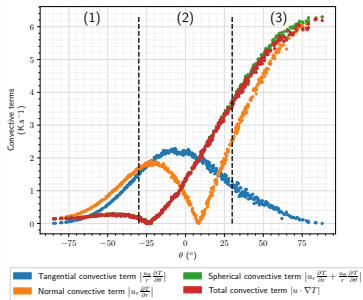
(a) Temperature ($D_b/\Delta = 64$, Fine)



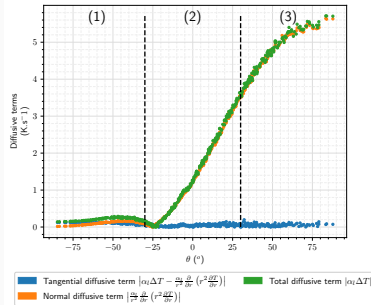
(b) Radial temperature gradient $\frac{\partial T}{\partial r}$

- ⇒ Strong variations observed at the bubble's top and equator regions.
- ⇒ Misprediction of the normal temperature gradient (Top and Equator regions):
30% relative error at $D_b/\Delta = 16$.

Highlighting the importance of tangential convective terms



(a) Convective terms (Fine)



(b) Diffusive terms (Fine)

THREE DISTINCT REGIONS:

- ⇒ Radial convection dominates in (1) and (3).
- ⇒ Tangential convective term gains importance in (2) (especially if Pr_t increases).
- ⇒ Radial diffusion dominates in (2) and (3).

Introduction

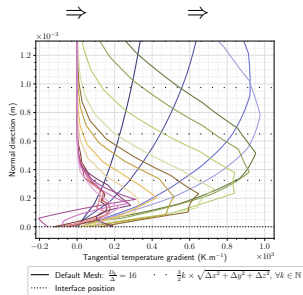
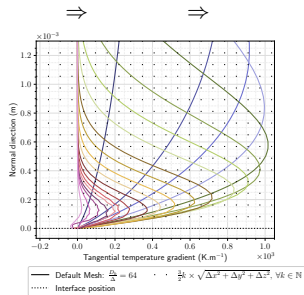
From available methods to a novel approach

LRS methodology

DNS simulations and post-processing tool

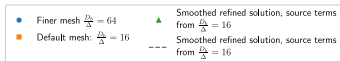
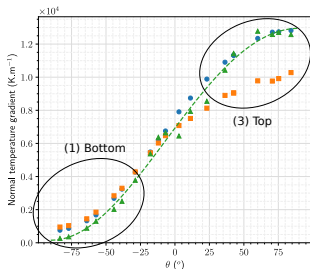
***A priori* implementation and results**

Conclusions and prospects

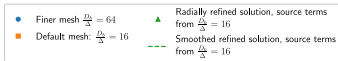
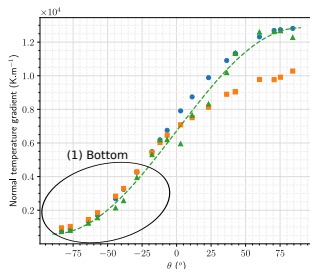
(a) $\frac{1}{r} \frac{\partial T}{\partial \theta}$, $D_b/\Delta = 16$ (b) $\frac{1}{r} \frac{\partial T}{\partial \theta}$, $D_b/\Delta = 64$

Case	Tangential terms	Figures of merit	
		Local interfacial gradient enhancement $\nabla T \cdot \mathbf{n}_\Gamma _\Gamma$	Nusselt number integrand dispersion $R_b^2 \nabla T \cdot \mathbf{n}_\Gamma _\Gamma \sin(\theta) d\theta d\phi \rightarrow Nu_b$ \int_Γ
A	C_{coarse}^θ ; $D_{\text{coarse}}^\theta = 0$	✓	
B	C_{coarse}^θ ; D_{coarse}^θ	✓	✓
C	C_{fine}^θ ; D_{fine}^θ		✓

Results for $Ar^* = 50$ and $Pr_l = 1$ ($Re_b \approx 62.5$)



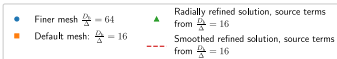
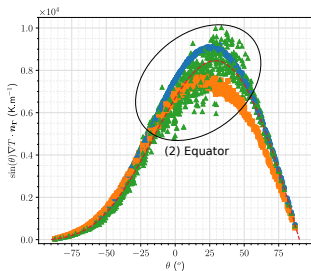
(a) Case A
 C_{coarse}^θ only



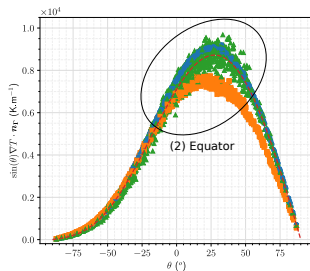
(b) Case B
 C_{coarse}^θ and D_{coarse}^θ

	Case A	Case B
(1) Bottom	Gradient underestimated	Coarse gradient value almost retrieved
(2) Equator	Values underestimated for $-5 < \theta < 25^\circ$	
(3) Top	Overall enhancement for $\theta > 25^\circ$	

Method's dispersion and global Nu_b convergence: $\nabla T \cdot \mathbf{n}_r|_{\Gamma} \sin(\theta)$



(a) Case B
 C_{coarse}^{θ} and D_{coarse}^{θ}



(b) Case C
 C_{fine}^{θ} and D_{fine}^{θ}

	Case B	Case C
(1) Bottom	Low dispersion	Reduce dispersion
(2) Equator	Dispersion is significant	Integral value underestimated
(3) Top	Precise and accurate prediction	

Nusselt number relative error (%)

Ar^*	Pr	Coarse Fine $\left(\frac{\Delta_{\text{fine}}}{\Delta_{\text{coarse}}}\right)^3$ Reference			$C_{\text{coarse}}^\theta, D_{\text{coarse}}^\theta$ Error (%)	$C_{\text{fine}}^\theta, D_{\text{fine}}^\theta$ Error (%)	
		$\frac{D_b}{\Delta}$	$\frac{D_b}{\Delta}$	error (%)			
1.0		16	64	64	16.06	8.67	3.61
50	2.5	22	90	68.5	19.46	8.61	1.53
	5.0	22	90	68.5	31.78	12.29	0.73

⇒ Enhancements using coarse (raw) source terms.

⇒ Tangential terms need a careful treatment.

Computational gain - Degrees of freedom

16 cells per diameter case:

1200 triangles & 32 points per sub-problem.

$$\underbrace{0.4 \text{ M}}_{D_b/\Delta=16} + \underbrace{38400}_{\text{Negligible}} \ll \underbrace{25 \text{ M}}_{D_b/\Delta=64} \quad (\text{Degrees of freedom})$$

LOCAL CONVERGENCE FOR HIGHER PECLET NUMBERS ($Re_b Pr_l = Pe_b = 400$)
BECOMES ACCESSIBLE FOR $D_b/\Delta \leq 40$.

Introduction

From available methods to a novel approach

LRS methodology

DNS simulations and post-processing tool

A priori implementation and results

Conclusions and prospects

Conclusions

- **A priori** assessment is promising at steady state.
- Tangential terms are too **significant** to be neglected!
- Error reduces drastically **16-32** → **8.7-12.3%** using **raw** CFD mesh quantities (Velocity u_r, u_θ , tangential terms $C_{\text{coarse}}^\theta, D_{\text{coarse}}^\theta$).



Achieved with **64** times less cells than the fine mesh.

- Extra-modelling of the tangential terms ($C_{\text{fine}}^\theta, D_{\text{fine}}^\theta$) could lead to higher enhancements.



<5% relative error on Nu_b .

- Method is suitable for any interface tracking methods (**FT-IBM**, Level-Set) / interface capturing methods (**VoF**)

Prospects

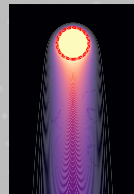
- Two way coupling and **a posteriori** assessment.
- 3D multi-bubbles column at moderate Peclet numbers ($Pe_b = Re_b Pr_l \leq 400$).














THANK YOU FOR YOUR ATTENTION !







KEYWORDS:

- Two-phase flow
- Ghost-fluid
- Boundary-Layer modelling
- DNS-Front-Tracking
- Heat transfer
- Sub-resolution approach



-  Aboulhasanzadeh, B. et al. (June 2012). “Multiscale computations of mass transfer from buoyant bubbles”. In: *Chemical Engineering Science* 75, pp. 456–467. DOI: [10.1016/j.ces.2012.04.005](https://doi.org/10.1016/j.ces.2012.04.005).
-  Aslam, T. D. (Jan. 2004). “A partial differential equation approach to multidimensional extrapolation”. In: *Journal of Computational Physics* 193.1, pp. 349–355. DOI: [10.1016/j.jcp.2003.08.001](https://doi.org/10.1016/j.jcp.2003.08.001).
-  Benarafa, Y. et al. (Apr. 2006). “RANS/LES coupling for unsteady turbulent flow simulation at high Reynolds number on coarse meshes”. In: *Computer Methods in Applied Mechanics and Engineering* 195.23-24, pp. 2939–2960. DOI: [10.1016/j.cma.2005.06.007](https://doi.org/10.1016/j.cma.2005.06.007). URL: <https://doi.org/10.1016/j.cma.2005.06.007>.
-  Bizid, W. (2017). “Développement de méthodes de pénalisation pour la simulation de l'écoulement turbulent autour d'obstacles”. PhD thesis. Université de Bordeaux.
-  Bothe, D. and S. Fleckenstein (Sept. 2013). “A Volume-of-Fluid-based method for mass transfer processes at fluid particles”. In: *Chemical Engineering Science* 101, pp. 283–302. DOI: [10.1016/j.ces.2013.05.029](https://doi.org/10.1016/j.ces.2013.05.029).
-  Chatelain, A. (2004). “Simulation des Grandes Echelles d'écoulements turbulents avec transferts de chaleur”. PhD thesis.

-  Fedkiw, R. P. et al. (July 1999). “A Non-oscillatory Eulerian Approach to Interfaces in Multimaterial Flows (the Ghost Fluid Method)”. In: *Journal of Computational Physics* 152.2, pp. 457–492. DOI: 10.1006/jcph.1999.6236. URL: <https://doi.org/10.1006/jcph.1999.6236>.
-  Feng, Z. and E. E. Michaelides (Dec. 2001). “Heat and mass transfer coefficients of viscous spheres”. In: *International Journal of Heat and Mass Transfer* 44.23, pp. 4445–4454. DOI: 10.1016/s0017-9310(01)00090-4. URL: [https://doi.org/10.1016/s0017-9310\(01\)00090-4](https://doi.org/10.1016/s0017-9310(01)00090-4).
-  Gibou, F., L. Chen, et al. (Mar. 2007). “A level set based sharp interface method for the multiphase incompressible Navier–Stokes equations with phase change”. In: *Journal of Computational Physics* 222.2, pp. 536–555. DOI: 10.1016/j.jcp.2006.07.035.
-  Gibou, F., R. P. Fedkiw, et al. (Feb. 2002). “A Second-Order-Accurate Symmetric Discretization of the Poisson Equation on Irregular Domains”. In: *Journal of Computational Physics* 176.1, pp. 205–227. DOI: 10.1006/jcph.2001.6977. URL: <https://doi.org/10.1006/jcph.2001.6977>.
-  Legendre, D., J. Borée, and J. Magnaudet (June 1998). “Thermal and dynamic evolution of a spherical bubble moving steadily in a superheated or subcooled liquid”. In: *Physics of Fluids* 10.6, pp. 1256–1272. DOI: 10.1063/1.869654.

-  Mathieu, B. (2003). “Études physique, expérimentale et numérique des mécanismes de base intervenant dans les écoulements diphasiques en micro-fluidique”. PhD thesis. Université de Provence.
-  Popinet, S. (2014). *Basilisk*. URL: <http://basilisk.fr>.
-  Tanguy, S. et al. (May 2014). “Benchmarks and numerical methods for the simulation of boiling flows”. In: *Journal of Computational Physics* 264, pp. 1–22. DOI: 10.1016/j.jcp.2014.01.014.
-  Vreman, A. W. (Apr. 2016). “Particle-resolved direct numerical simulation of homogeneous isotropic turbulence modified by small fixed spheres”. In: *Journal of Fluid Mechanics* 796, pp. 40–85. DOI: 10.1017/jfm.2016.228.
-  Weiner, A. (2020). “Modeling and simulation of convection-dominated species transfer at rising bubbles”. PhD thesis. Technical University of Darmstadt.
-  Weiner, A. and D. Bothe (Oct. 2017). “Advanced subgrid-scale modeling for convection-dominated species transport at fluid interfaces with application to mass transfer from rising bubbles”. In: *Journal of Computational Physics* 347, pp. 261–289. DOI: 10.1016/j.jcp.2017.06.040.



Zhao, S., J. Zhang, and M. Ni (Dec. 2021). “Boiling and evaporation model for liquid-gas flows: A sharp and conservative method based on the geometrical VOF approach”. In: *Journal of Computational Physics*, p. 110908. DOI: [10.1016/j.jcp.2021.110908](https://doi.org/10.1016/j.jcp.2021.110908).

Mass, momentum and energy conservation in conservative form

The continuous local and instantaneous system of equations used to describe two-phase flows with phase is given by:

$$\nabla \cdot \mathbf{u} = -\dot{m}_v \left(\frac{1}{\rho_v} - \frac{1}{\rho_l} \right) \delta_\Gamma \quad (3a)$$

$$\begin{aligned} \partial_t(\rho \mathbf{u}) + \nabla \cdot (\rho \mathbf{u} \otimes \mathbf{u}) \\ = \nabla \cdot (p \mathbf{I} + \mathcal{D}_u) + \rho \mathbf{g} + \kappa \sigma \mathbf{n}_v \delta_\Gamma \end{aligned} \quad (3b)$$

$$\begin{aligned} \partial_t(\rho C_p T) + \nabla \cdot (\rho C_p \mathbf{u} T) \\ = \nabla \cdot (\lambda \nabla T) + \dot{m}_v \delta_\Gamma \mathcal{L}^{vap} \end{aligned} \quad (3c)$$

$$\partial_t \chi_v + \mathbf{u}_\Gamma \cdot \nabla \chi_v = 0 \quad (3d)$$

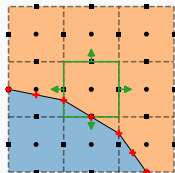
$$T_\Gamma = T^{sat} = \text{const} \quad (3e)$$

$$\mathbf{u}_\Gamma = \mathbf{u}_l - \frac{\dot{m}_v}{\rho_l} \mathbf{n}_v \quad (3f)$$

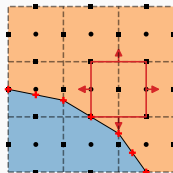
$$\dot{m}_v = \rho_v (\mathbf{u}_v - \mathbf{u}_\Gamma) \cdot \mathbf{n}_\Gamma \quad (3g)$$

It remains true in the sense of the distribution (Dirac δ "function"). The discontinuity is embedded in the discretised field.

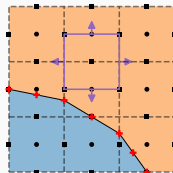
Discretisation: Marker and cells/Staggered grid



Continuity - Scalar



X velocity Momentum



Y velocity Momentum

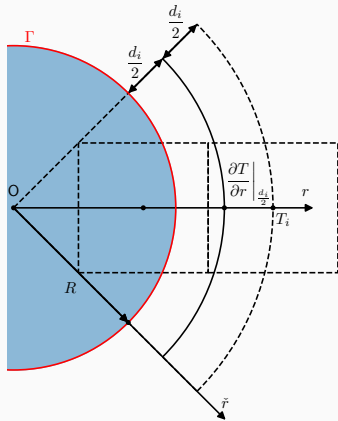
Curvature calculation: differential approach of Mathieu 2003

$$\kappa = -\frac{\mathbf{n}_{\Gamma}^S \cdot \mathbf{n}_{\Gamma}^V}{\mathbf{n}_{\Gamma}^V \cdot \mathbf{n}_{\Gamma}^V} = -\frac{\frac{\partial S}{\partial x} \frac{\partial V}{\partial x} + \frac{\partial S}{\partial y} \frac{\partial V}{\partial y}}{\left(\frac{\partial V}{\partial x}\right)^2 + \left(\frac{\partial V}{\partial y}\right)^2} \quad (4)$$

$$dV = \left(\frac{\partial V}{\partial x}, \frac{\partial V}{\partial y}\right) \cdot (dx, dy) = \mathbf{n}_{\Gamma}^V \cdot d\mathbf{x}_i \quad (5a)$$

$$dS = \left(\frac{\partial S}{\partial x}, \frac{\partial S}{\partial y}\right) \cdot (dx, dy) = \mathbf{n}_{\Gamma}^S \cdot d\mathbf{x}_i \quad (5b)$$

Sub-grid diffusion model and spreading procedure



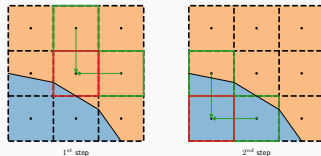
(a) Temperature gradient evaluation:

$$\frac{\partial T}{\partial r} \Big|_{R+d_i/2}^{\text{num}} \xrightarrow{\text{Sub-grid diffusion}} \frac{\partial T}{\partial r} \Big|_{\Gamma}$$

- Compute normal vectors \mathbf{n} , distance function d , curvature κ .
- Second order evaluation of gradient at $\tilde{r} = R + d_i/2$.
- Sub-grid model to evaluate the gradient at the interface.

$$\Delta_{sph} T \approx \kappa \frac{\partial T}{\partial r} + \frac{\partial^2 T}{\partial r^2} = 0 \quad (6)$$

- Extend temperature with same analytical expression.



(b) Spreading procedure. Stored values are initially in pure cells.

Differences with the literature

Literature:

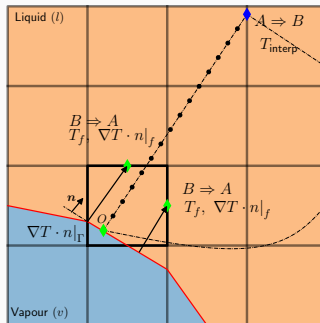
- Aslam's n^{th} order extrapolation (Aslam 2004)
 - ⇒ Extrapolate each derivative iteratively on a pseudo-time step τ .
 - ⇒ Starting from $\frac{\partial^n T}{\partial r^n}$ and ending with zero order derivative *i.e.* T .
- Implicit diffusion
 - ⇒ Impose the saturation temperature $T_\Gamma = T^{sat}$ in the diffusion matrix taking into account the interface position (Gibou, Fedkiw, et al. 2002; Gibou, Chen, et al. 2007; Tanguy et al. 2014).

TrioCFD methods:

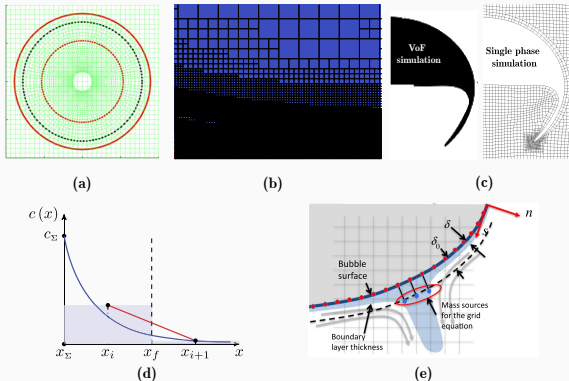
- Extended field T^{ext} verifying $T_\Gamma = T^{sat}$.
- Updated temperature field T^{n+1} does not ensure saturation temperature condition.
- Explicit diffusion.

Coupling with the resolved field

- Eulerian (A) \Rightarrow Boundary layer (B)
 - \Rightarrow Local temperature value(s) (Fitting, B.Cs).
- (B) Boundary layer \Rightarrow Eulerian (A)
 - \Rightarrow Interfacial temperature gradient correction $\nabla T \cdot \mathbf{n}_\Gamma$.
 - \Rightarrow Temperature and fluxes correction on faces f : $T_f, \nabla T \cdot \mathbf{n}_\Gamma|_f$.

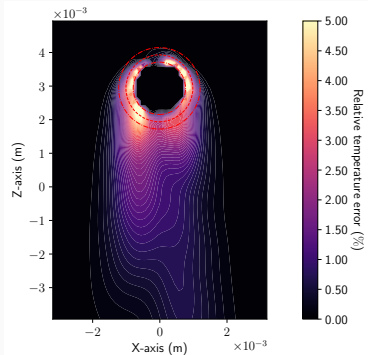


Various numerical approaches to enhance predictions of strong variations

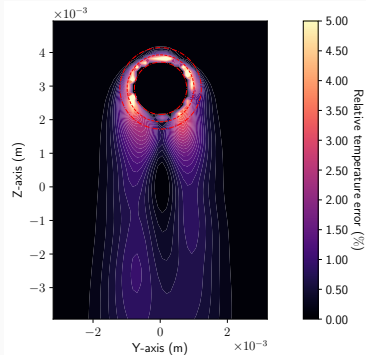


- (a) Particle-attached mesh in polar coordinates (2D) from Vreman 2016
- (b) Adaptive Mesh Refinement from Popinet 2014; Zhao, Zhang, and Ni 2021
- (c) VoF to single-phase simulation framework developed by Weiner 2020
- (d) Analytical profile fitted on the first mesh average concentration value: quasi-static approach of Weiner and Bothe 2017
- (e) Unsteady boundary layer tracking approach Aboulhasanzadeh et al. 2012

Temperature error field at $Ar^* = 50$, $Pr_l = 1$. ($Re_b = 62.5$)

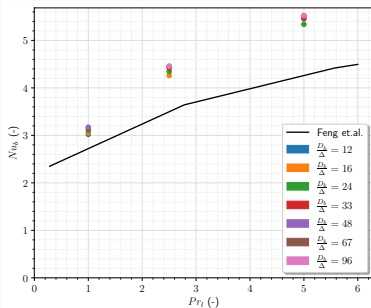
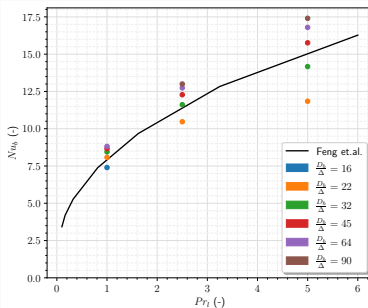


(a) $D_b/\Delta = 16$



(b) $D_b/\Delta = 64$

Error is less than 5% on average. The error made at the interface is not propagating significantly through the domain. It reinforces our trust in an *a priori* methodology.

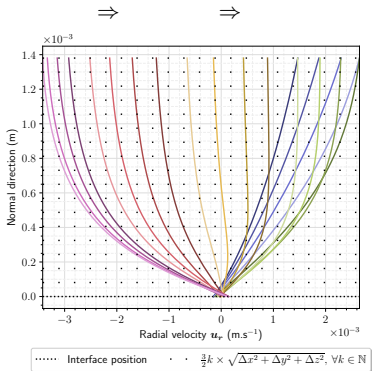
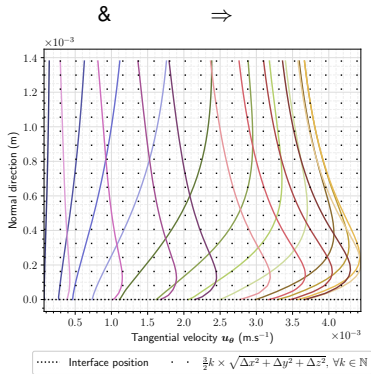
Nusselt number values for increasing spatial resolution D_b/Δ (a) $Ar^* = 10$, $Re_b \approx 3.6$ (b) $Ar^* = 50$, $Re_b \approx 62.5$

(a) Nusselt number converges rapidly to the reference solution, (b) Nusselt number prediction depends clearly on the Prandtl number. Correlations Eq.(29a) from Feng and Michaelides 2001

Increase in liquid Prandtl number $Pr_l = \frac{\alpha_l}{\nu_l}$:

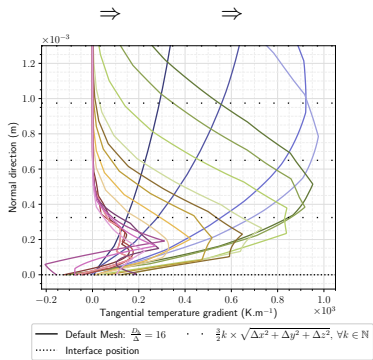
⇒ Thermal boundary layer gets **thinner**

⇒ Spatial resolution requirements increases linearly *i.e.* $Pr_l \times 2 \rightarrow \Delta_{x,y,z} \times 2 \rightarrow N_{cells} \times 8$

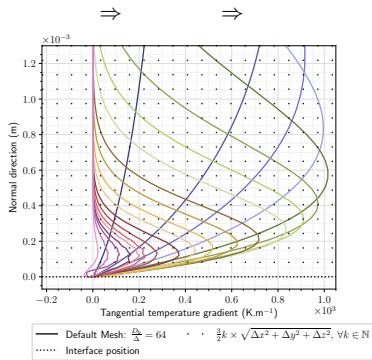
(a) Radial velocity u_r (b) Tangential velocity u_θ

- ⇒ u_r profiles are **linear** in the radial direction.
- ⇒ u_r is cancelling approximately at the interface for numerical reasons. (viscosity calculation favouring one of the two phases and offset "virtually" the point of zero velocity)
- ⇒ u_θ profiles are **non-linear** in the radial direction.

Tangential temperature derivative $\nabla T \cdot \tilde{e}_\theta = \frac{1}{r} \frac{\partial T}{\partial \theta}$

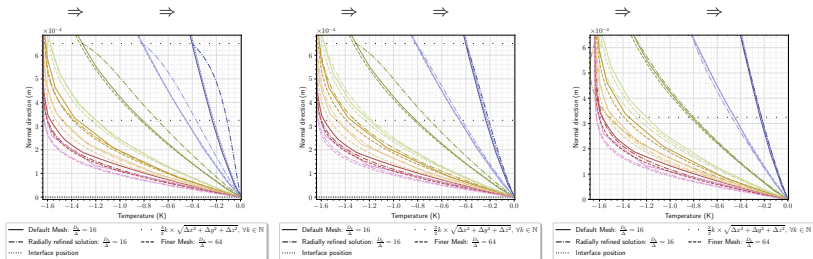


(a) $D_b/\Delta = 16$



(b) $D_b/\Delta = 64$

- ⇒ Post-processed tangential derivative term is very **noisy** for $D_b/\Delta = 16$.
- ⇒ Not well captured even if less significant !
- ⇒ Zero tangential n^{th} order derivatives imposed implicitly by $T_\Gamma = T^{sat}$.
- ⇒ **Modelling** this term could be interesting.

(a) Case A - $C_{\text{coarse}}^{\theta}$ (b) Case B - $C_{\text{coarse}}^{\theta}, D_{\text{coarse}}^{\theta}$ (c) Case F - $C_{\text{fine}}^{\theta}, D_{\text{fine}}^{\theta}$

	Case A	Case B	Case F
(1)	Wrong sign of $\nabla T \cdot n_{\Gamma} _{\text{end}}$	Gradient error reduced at the bottom	Coherent with coarse and fine solutions
(2)	Not a clear enhancement		Enhancements close to the interface
(3)		Clear enhancement over the probe length	Discrepancies observed at the probes'end

Regularised profiles

Levich-Ruckenstein regularised profiles employed by Legendre, Borée, and Magnaudet 1998:

$$\frac{\nabla T \cdot \mathbf{n}_\Gamma(\theta)}{\nabla T \cdot \mathbf{n}_\Gamma|_{\theta=\pi/2}} = \frac{\sqrt{a} \cos^2\left(\frac{\pi/2-\theta}{2}\right)}{\sqrt{(a-1) + \cos(\pi/2-\theta)}} + b; \quad a^{th} = 2; b^{th} = 0 \quad (7)$$

Nusselt number formula ($r = R_b$)

$$Nu_b = D_b R_b^2 / \Delta T \int_{S_\Gamma} \underbrace{\nabla T \cdot \mathbf{n}_\Gamma|_\Gamma \sin(\theta)}_{\text{Integrand}} d\theta d\phi \quad (8)$$

Where ϕ varies between 0 and 2π and θ between 0 and π .

Perspectives and questions

- Operators straddling the interface should be adapted:
 - ⇒ **Split** the two phases' resolution (Forget about Ghost Fluid Methods?).
- Applicability to condensing bubbles:
 - ⇒ Effets of the **velocity jump** \dot{m}_v , $Ja \neq 0$?
 - ⇒ Same treatment for the velocity ?
- A multi-bubbles column configuration aimed in the thesis:
 - ⇒ **Quasi-Static** approach still relevant ?
 - ⇒ Will thermal boundary layers **perturbations** are fast ?

WILL DISCONTINUOUS NUMERICAL TREATMENTS OF QUANTITIES
OVERCOME DIFFUSE METHODS ?